Fluctuating pulse propagation in resonant nonlinear media: self-induced transparency random phase soliton formation

Laleh Mokhtarpour* **and Sergey A. Ponomarenko**

Department of Electrical and Computer Engineering, Dalhousie University, Halifax, NS, B3J 2X4 Canada

Laleh.Mkht@dal.ca

Abstract: We numerically investigate partially coherent short pulse propagation in nonlinear media near optical resonance. We examine how the pulse state of coherence at the source affects the evolution of the ensemble averaged intensity, mutual coherence function, and temporal degree of coherence of the pulse ensemble. We report evidence of self-induced transparency random phase soliton formation for the relatively coherent incident pulses with sufficiently large average areas. We also show that random pulses lose their coherence on propagation in resonant media and we explain this phenomenon in qualitative terms.

OCIS codes: (030.0030) Coherence and statistical optics; (260.5740) Resonance; (190.5530) Pulse propagation and temporal solitons; (320.7110) Ultrafast nonlinear optics; (320.5550) Pulses.

References and links

1. R. W. Boyd, *Nonlinear Optics* (Academic Press, 2008).
2. P. P. Banerjee, *Nonlinear Optics: Theory, Numerical Modeling and Applications* (Marcel Decker, 2004).
3. S. A. Ponomarenko and G. P. Agrawal, "Linear optical bullets," Opt. Commun. **261**, 1–4 (2006).
4. G. P. Agrawal, *Nonlinear Fiber Optics* (Academic Press, 2007).
5. M. Bertolotti, A. Ferrari, and L. Sereda, "Coherence properties of nonstationary polychromatic light sources," J. Opt. Soc. Am. B **12**, 341–347 (1995).
6. L. Sereda, M. Bertolotti, and A. Ferrari, "Coherence properties of nonstationary light wave fields," J. Opt. Soc. Am. B **15**, 695–705 (1998).
7. H. Lajunen, J. Tervo, J. Turunen, P. Vahimaa, and F. Wyrowski, "Spectral coherence properties of temporarily modulated stationary light sources," Opt. Express **11**, 1894–1899 (2003).
8. L. Ma and S. A. Ponomarenko, "Optical coherence gratings and lattices," Opt. Lett. **39**, 6656 (2014).
9. P. Paakkonen, J. Turunen, P. Vahimaa, A. T. Friberg, and F. Wyrowski, "Partially coherent Gaussian pulses," Opt. Commun. **204**, 53–58 (2002).
10. S. A. Ponomarenko, G. P. Agrawal, and E. Wolf, "Energy spectrum of a nonstationary ensemble of pulses," Opt. Lett. **29**, 394–396 (2004).
11. P. Vahimaa and J. Turunen, "Independent-elementary-pulse representation for non-stationary fields," Opt. Express **14**, 5007–5012 (2006).
12. S. A. Ponomarenko, "Complex Gaussian representation of statistical pulses," Opt. Express **19**, 17086–17091 (2011).
13. Q. Lin, L. Wang, and S. Zhu, "Partially coherent light pulse and its propagation," Opt. Commun. **219**, 65–70 (2003).
14. M. Brunel and S. Coëtlemec, "Fractional-order Fourier formulation of the propagation of partially coherent light pulses," Opt. Commun. **230**, 1–5 (2004).
15. W. Huang, S. A. Ponomarenko, M. Cada, and G. P. Agrawal, "Polarization changes of partially coherent pulses propagating in optical fibers," J. Opt. Soc. Am. A **24**, 3063–3068 (2007).

#249844 Received 9 Sep 2015; revised 4 Nov 2015; accepted 5 Nov 2015; published 11 Nov 2015

16. R. W. Schoonover, B. J. Davis, R. A. Bartels, and P. S. Carney, "Propagation of spatial coherence in fast pulses," J. Opt. Soc. Am. A **26**, 1945–1953 (2009).
17. C. L. Ding, L. Z. Pan, and B. D. Lu, "Changes in the spectral degree of polarization of stochastic spatially and spectrally partially coherent electromagntic pulses in dispersive media," J. Opt. Soc. Am. B **26**, 1728–1735 (2009).
18. S. A. Ponomarenko, "Degree of phase-space separability of statistical pulses," Opt. Express **20**, 2548–2555 (2012).
19. S. A. Ponomarenko, "Self-imaging of partially coherent light in graded-index media," Opt. Lett. **40**, 566 (2015).
20. B. Gross and J. T. Manassah, "Compression of the coherence time of incoherent signals to a few femto seconds," Opt. Lett. **16**, 1835–1837 (1991).
21. V. A. Aleshkevich, V. A. Vysloukh, G. D. Kozhoridze,A. N. Matveev and S. I. Terzieva, "Nonlinear propagation of partially coherent pulse in fiber waveguide and the role of higher order dispersion," Sov. J. Quantum Electron. **18**, 207–211 (1988).
22. S. B. Cavalcanti, G. P. Agrawal and M. Yu, " Noise amplification in dispersive nonlinear media," Phys. Rev. A **51**, 4086–4092 (1995).
23. H. Lajunen, V. Torres-Company, J. Lancis, E. Silvestre, and P. Andrés, "Pulse-by-pulse method to characterize partially coherent pulse propagation in instantaneous nonlinear media," Opt. Express **18**, 14979–14991 (2011).
24. L. Mokhtarpour and S. A. Ponomarenko, "Complex area correlation theorem for statistical pulses in coherent linear absorbers," Opt. Lett. **37**, 3498–3500 (2012).
25. L. Mokhtarpour and S. A. Ponomarenko, "Ultrashort pulse coherence properties in coherent linear amplifiers," J. Opt. Soc. Am. A **30**, 627–630 (2013).
26. L. Mokhtarpour, G. H. Akter, and S. A. Ponomarenko, "Partially coherent self-similar pulses in resonant linear absorbers," Opt. Express **20**, 17816–17822 (2012).
27. L. Allen and J. H. Eberly, *Optical Resonance and Two-level Atoms* (Dover, 1975).
28. J. C. Diels and W. Rudolph, *Ultrashort Laser Pulse Phenomena* (Academic Press, 2006)
29. L. Banyai and S. W. Koch, *Semiconductor Quantum Dots* (World Scientific, 1993).
30. Y. Wu and L. Deng, "Ultraslow bright and dark optical solitons in a cold three-state system," Opt. Lett. **29**, 2064–2066 (2004).
31. C. Hang and G. Huang, "Giant Kerr nonlinearity and weak-light superluminal optical solitons in a four-state atomic system with gain doublet," Opt. Express **18**, 2952–2966 (2010).
32. W-X. Yang, Ai-Xi Chen, L-G. Si, K. Jiang, X. Yang, and R-K. Lee, "Three coupled ultraslow solitons in a five-level tripod system," Phys. Rev. A **81** 023814 (2010).
33. L. Mandel and E. Wolf, *Optical Coherence and Quantum Optics* (Cambridge University, 1997).
34. S. A. Ponomarenko and E. Wolf, "Coherence properties of light in Young's interference pattern formed with partially coherent light," Opt. Commun. **170**, 1–8 (1999).
35. S. A. Ponomarenko, H. Roychoudhury, and E. Wolf, "Physical significance of complete spatial coherence of optical fields," Phys. Lett. A, **345**, 10–12 (2005).
36. S. A. Ponomarenko and E. Wolf, "The spectral degree of coherence of fully spatially coherent electromagnetic beams," Opt. Commun. **227**, 73–74 (2003).
37. A. S. Monin and A. M. Yaglom, *Statistical Fluid Mechanics: Mechanics of Turbulence*, Vols. 1& 2, (Dover, 2007).
38. G. A. Pasmanik, "Self-interaction of incoherent light beams," Sov. Phys. JETP, **39**, 234–238 (1974).
39. M. Mitchell, M. Segev, T. H. Coskun, and D. N. Christodoulides, "Theory of Self-Trapped Spatially Incoherent Light Beams," Phys. Rev. Lett. **79**, 4990–4993 (1997).
40. D. N. Christodoulides, E. D. Eugenieva, T. H. Coskun, M. Segev, and M. Mitchell, "Equivalence of three approaches describing partially incoherent wave propagation in inertial nonlinear media," Phys. Rev. E **63**, 035601(R) (2001).
41. S. A. Ponomarenko, N. M. Litchinitser, and G. P. Agrawal, "Theory of incoherent solitons: Beyond the mean-field approximation," Phys. Rev. E **70**, 015603(R) (2004).
42. V. P. Kandidov, "Monte Carlo method in nonlinear statistical optics", Sov. Phys.Usp. **39**, 1243–1272 (1996).
43. X. Xiao and D. Voelz, "Wave optics simulation approach for partial spatially coherent beams," Opt. Express **16**, 6986–6992 (2006).
44. S. A. Parhl, D. G. Fischer and D. D. Duncan, "Monte Carlo Green's function for the propagation of partially coherent light," J. Opt. Soc. Am. A **260**, 1533–1543 (2009).
45. E. Wolf,"New spectral representation of random sources and of the partially coherent fields that they generate," Opt. Commun. **38**, 3–6 (1981).
46. F. Gori, "Collett-Wolf sources and multimode lasers," Opt. Commun. **34**, 301–305 (1980).
47. A. Starikov and E. Wolf, "Coherent-mode representation of Gaussian Schell-model sources and of their radiation fields," J. Opt. Soc. Am. A **72**, 923–928 (1982).
48. P. W. Milonni and J. H. Eberly, *Lasers* (Wiley, 1985).

#249844 Received 9 Sep 2015; revised 4 Nov 2015; accepted 5 Nov 2015; published 11 Nov 2015

1. Introduction

The invention of lasers and their wide range of applications to optical communication systems has led to a growing interest in the field of nonlinear optics, which explores modifications of optical properties of the host media upon interaction with high intensity temporal and spatio-temporal pulses [1–3]. A proper description of realistic laser pulses - with inevitable fluctuations in their amplitude, phase, and width - cannot be achieved without the aid of statistical optics. Moreover, the limitations that noise in ultrashort laser pulses imposes on the performance of optical communication systems have triggered an ever growing interest in coherence properties of ultrashort pulses [4].

Following the pioneering work of Bertolotti's group [5, 6], comprehensive research has been carried out on various aspects of partially coherent sources [7, 8] and the pulses generated by such sources [9, 10]. Further, several theoretical approaches to the description of partially coherent pulses have been proposed to date [11, 12]. The evolution of coherence and polarization state of partially coherent pulses in generic linear [13–19] and nonlinear [20–23] dispersive media far from any internal resonances has been thoroughly examined using various mathematical techniques.

At the same time, coherence properties of generic partially coherent pulses traveling in resonant linear absorbers and amplifiers have been analyzed [24, 25] and their coherence function modifications upon propagation investigated. Furthermore, the crucial impact of the initial coherence level of random pulses on their self-similar propagation in resonant linear absorbers has been established [26]. To our knowledge, however, no study of partially coherent pulse propagation in resonant nonlinear media has yet been attempted. The subject naturally arises in the context of short intense pulse interaction with atomic vapours [27], impurity doped solids [28], or semiconductor quantum dot media [29] near resonance whenever pulse fluctuations cannot be neglected.

In this work, we fill in the gap by numerically studying short random pulse propagation in resonant nonlinear media in the two-level approximation. We examine the behaviour of the ensemble averaged intensity, mutual coherence function, and temporal degree of coherence for pulses with relatively large and relatively small average areas. We explore the influence of the coherence state at the source on ensuing pulse evolution scenarios. We reveal evidence of self-induced transparency random phase soliton formation for rather coherent large-area input pulses. We stress that although soliton formation in resonant nonlinear media has been extensively studied either in the two-level [27] or multi-level [30–32] approximation, the work in this direction has so far focused on fully temporarily coherent solitons. We also show that all pulses lose their coherence on propagation in such media, regardless of their initial state of coherence. Yet, the coherence loss rate on propagation is strongly affected by the pulse coherence level at the source: the lower the source coherence, the greater the coherence loss rate. Our results are applicable to a multitude of resonant media, including dilute atomic vapours filling the hollow-core photonic crystal fibres, impurity-doped solids, and semiconductor quantum dots in the strong quantum confinement regime.

2. Pulse propagation in resonant nonlinear media

In this work, we model resonant optical media as a collection of two-level atoms. In particular, we describe the light-matter interactions within the framework of the Maxwell-Bloch equations [27]. The fluctuating pulse evolution in the medium can then be described in the slowly-varying envelope approximation by the reduced wave equation in the transformed coordinates, $\zeta = z$ and $\tau = t - z/c$, as

$$\partial_\zeta \Omega = \frac{i}{2} \frac{\omega N |d_{eg}|^2}{c\varepsilon_0 \hbar} \overline{\sigma}_\Delta. \tag{1}$$

#249844 Received 9 Sep 2015; revised 4 Nov 2015; accepted 5 Nov 2015; published 11 Nov 2015

In Eq. (1), $\Omega = 2d_{eg}\mathscr{E}/\hbar$ is the Rabi frequency corresponding to the field envelope $\mathscr{E}$. Hereafter, we will find it convenient to express the electric field envelope in frequency units employing the Rabi frequency Ω instead of the field envelope $\mathscr{E}$.Also, N is the atom density, and d_{eg} is the dipole matrix element between the nondegenerate ground and excited states of an atom. Also, $\overline{\sigma}_\Delta$ denotes the dipole envelope function of an atomic dipole moment averaged over a distribution of detunings Δ of the carrier wave frequency ω from the atomic resonance frequency ω_0,

$$\overline{\sigma_\Delta} = \int d\Delta g(\Delta)\sigma(\Delta). \tag{2}$$

Here, $g(\Delta)$ is assumed as the inhomogeneous broadening function with Gaussian distribution

$$g(\Delta) = \frac{1}{\sqrt{2\pi}\delta}\exp\left(-\frac{\Delta^2}{2\delta^2}\right), \tag{3}$$

in which δ represents the inhomogeneous broadening width.

Next, the Bloch equations governing the complex dipole envelope function σ and one-atom inversion w dynamics can be expressed in the form [27]

$$\partial_\tau\sigma = -(\tfrac{1}{T_\perp} + i\Delta)\sigma - i\Omega w, \tag{4}$$

and

$$\partial_\tau w = -\tfrac{1}{T_{||}}(w+1) - \tfrac{i}{2}(\Omega^*\sigma - \Omega\sigma^*). \tag{5}$$

Here, $T_\perp$ and $T_{||}$ are the dipole phase and atomic population relaxation times, respectively.

To explore the feasibility of self-induced transparency phenomena, we need to consider coherent transient regime in that the input pulse width is so short ($t_p < min(T_\perp, T_{||})$) that atoms of the material undergo no damping during their interaction with the pulse. Therefore, the evolution of atomic variables can be studies as if no damping effect is present. In such a case the Bloch equations reduce to

$$\partial_T\sigma = -i\Delta\sigma - i\Omega w, \tag{6}$$

$$\partial_T w = -\tfrac{i}{2}(\Omega^*\sigma - \Omega\sigma^*). \tag{7}$$

Here, $Z = \alpha\zeta$ and $T = t/t_p$, t_p denoting a characteristic rms width of the incident pulse, are dimensionless variables and, $\alpha = N|d_{eg}|^2\omega^2/\sqrt{2\pi}\delta\hbar\varepsilon_0 c^2$ represents the linear absorption coefficient.

To quantitatively describe the pulse evolution in the medium, we must, in general, numerically solve the Maxwell-Bloch equations, Eqs. (1)-(3), together with Eqs.(6)-(7) subject to the appropriate initial and boundary conditions. We assume that the atoms are all initially in their ground states such that $\sigma = 0$ and $w = -1$, and the source field envelope $\Omega(t,0)$ (in the frequency units) is known. However, as incident pulses have fluctuating amplitudes and phases, we can only describe the pulse evolution in terms of appropriate correlation functions.

3. Statistical properties of fluctuating pulses and statistical ensemble generation

Henceforth, we will be primarily interested in the second-order temporal coherence properties of fluctuating pulses, propagating in resonant nonlinear media. The latter are specified by the second-order cross-correlation function, defined as

$$\Gamma(\tau_1, \tau_2, \zeta) = \langle\Omega^*(\tau_1, \zeta)\Omega(\tau_2, \zeta)\rangle, \tag{8}$$

where the angle brackets denote ensemble averaging over all possible field realizations. The ensemble power distribution is then defined in terms of the average intensity as

$$I(\tau, \zeta) \equiv \Gamma(\tau, \tau, \zeta), \tag{9}$$

#249844 Received 9 Sep 2015; revised 4 Nov 2015; accepted 5 Nov 2015; published 11 Nov 2015

and the ensemble coherence properties are characterized by the temporal degree of coherence [33, 34]

$$\gamma(\tau_1,\tau_2,\zeta) \equiv \frac{\Gamma(\tau_1,\tau_2,\zeta)}{\sqrt{I(\tau_1,\zeta)I(\tau_2,\zeta)}}. \tag{10}$$

In the fully coherent limit, the degree of coherence attains its maximum, $|\gamma(\tau_1,\tau_2,\zeta)| = 1$ [33, 35, 36].

The description of fluctuating field propagation in nonlinear media directly in terms of the correlation functions runs into a formidable obstacle known as a closure problem which emerges regardless of the nonlinearity nature, see, for instance [37]. It can be shown that whenever one attempts to derive an equation of motion for the second-order correlation functions using the Maxwell-Bloch equations, the resulting equation will also involve third-order correlations. The corresponding evolution equations for the third-order correlation functions will depend on fourth-order correlations and so forth, resulting in an infinite hierarchy of the evolution equations for correlation functions of all orders. One is then forced to either neglect correlation functions higher than a certain order or make ad hoc assumptions regarding the pulse statistics that make it possible to express higher-order correlations in terms of the lower-order ones. This dilemma is known as a closure problem. In general, neither resolution of the dilemma has been shown to yield satisfactory results for realistic nonlinear media [37] unless the medium response time is much longer than a characteristic coherence time of the incident field. In the latter case, the medium averages over higher-order field fluctuations and a mean-field [38–40] or averaged-response description [41] is possible leading to a closed form evolution equation for the second-order correlation function. In the present case, the resonant medium response is noninstantaneous, but the response time can be either longer or shorter than the pulse coherence time. Thus, the closure problem cannot be easily resolved and we must resort to a different mathematical description.

To this end, we employ a wave optical Monte Carlo method which was developed in [42–44] and recently applied to random pulse propagation in nonresonant media with Kerr nonlinearities [23]. In essence, the technique entails generating an ensemble $\{\Omega(t)\}$ of random fluctuating pulses at the source with specified coherence properties and transmitting individual ensemble realizations through the resonant medium. At the end, the ensemble average is performed and the appropriate second-order correlation functions are determined. Thus, we first have to solve the Maxwell-Bloch equations Eqs.(1)-(3) and Eqs.(6)-(7) numerically for each random realization of the pulse and then average over L members of the ensemble according to

$$\Gamma_L(\tau_1,\tau_2,\zeta) = \frac{1}{L}\sum_{i=1}^{L} \Omega^*(\tau_1,\zeta)\Omega(\tau_2,\zeta), \tag{11}$$

to obtain the second-order cross-correlation function of the pulse ensemble. The averaged degree of coherence of the ensemble is then determined by

$$\gamma_L(\tau_1,\tau_2,\zeta) = \frac{\Gamma_L(\tau_1,\tau_2,\zeta))}{\sqrt{I_L(\tau_1,\zeta)I_L(\tau_2,\zeta)}}. \tag{12}$$

To construct the pulse ensemble, we begin by representing a fluctuating field in any transverse plane $\zeta \geq 0$ through the Karhunen-Loève expansion as

$$\Omega(\tau,\zeta) = \sum_n a_n \psi_n(\tau,\zeta), \tag{13}$$

where $\{a_n\}$ are uncorrelated random amplitudes, and $\{\psi_n(\tau,\zeta)\}$ are orthogonal coherent modes. We specify a non-Gaussian pulse ensemble statistics through

$$a_n = \sqrt{\lambda_n}\exp(i\varphi_n), \tag{14}$$

#249844 Received 9 Sep 2015; revised 4 Nov 2015; accepted 5 Nov 2015; published 11 Nov 2015

where $\{\varphi_n\}$ are statistically independent random phases, uniformly distributed in the interval $[-\pi,\pi]$ [23]. The statistical independence of the set $\{\varphi_n\}$ implies that

$$\langle \exp[i(\varphi_n - \varphi_m)]\rangle = \delta_{mn}, \tag{15}$$

Notice that the statistics (14), together with (15), imply that

$$\langle a_n^* a_m\rangle = \lambda_n \delta_{mn}. \tag{16}$$

Assuming the modes are normalized at the source, each λ_n determines the power carried by the nth mode of the source.

It then follows at once from Eqs. (13) and (16) as well as the definition of Γ, Eq. (8), that [45]

$$\Gamma(\tau_1,\tau_2,\zeta) = \sum_n \lambda_n \psi_n^*(\tau_1,\zeta)\psi_n(\tau_2,\zeta). \tag{17}$$

Here λ_n and $\psi_n(\tau,\zeta)$ are the eigenvalues and eigenmodes of the Fredholm integral equation,

$$\int_{-\infty}^{\infty} d\tau_1\, \Gamma(\tau_1,\tau_2,\zeta)\psi_n(\tau_1,\zeta) = \lambda_n \psi_n(\tau_2,\zeta). \tag{18}$$

It remains to specify the second-order correlations of the source which determine the coherent modes and their weights. To this end, we employ a generic Gaussian Schell-model (GSM) source with the cross-correlation function

$$\Gamma(t_1,t_2) = \frac{E}{\sqrt{\pi}t_\mathrm{p}} \exp\left[-\frac{(t_1^2+t_2^2)}{2t_\mathrm{p}}\right] \exp\left[-\frac{(t_1-t_2)^2}{2t_\mathrm{c}^2}\right], \tag{19}$$

where t_p and t_c are characteristic pulse width and coherence time at the source and E is a total energy of the source. The coherent modes of GSM sources are analytically known [46, 47] as

$$\psi_n(t) = \frac{1}{\sqrt{2^n n!}} \left(\frac{2\pi}{d}\right)^{1/4} H_n\left(\frac{t}{\sqrt{2d}}\right) \exp\left(-\frac{t^2}{4d}\right), \tag{20}$$

where $H_n(t)$ is a Hermite polynomial of order n. The modal weights are given by

$$\lambda_n = \left(\frac{\pi}{a+b+d}\right)^{1/2} \left(\frac{b}{a+b+d}\right)^n. \tag{21}$$

The parameters a,b and d are defined as

$$a = \frac{t_\mathrm{p}^2 t_\mathrm{c}^2}{2(t_\mathrm{c}^2+2t_\mathrm{p}^2)}, \qquad b = \frac{t_\mathrm{p}^4}{2(t_\mathrm{c}^2+2t_\mathrm{p}^2)}, \tag{22}$$

and

$$d = \sqrt{a^2+2ab}. \tag{23}$$

where t_p and t_c correspond to the characteristic width and coherence time of the pulse respectively [7, 9]. The coherence time, t_c specifies a time duration over which two pulses can be added coherently. The limits $t_c = 0$ and $t_c = \infty$ correspond to uncorrelated and fully correlated pulses, respectively.

In proceeding with modeling random sample pulses, we ascertain here a proper definition for the variable a_n in Eq. (14).

#249844 Received 9 Sep 2015; revised 4 Nov 2015; accepted 5 Nov 2015; published 11 Nov 2015

As we are interested in simulating noisy laser pulses, we generate an ensemble with non-Gaussian statistics. To do so, the random phases φ_n in Eq. (14), are chosen to be uniformly distributed in the interval $[-\pi, \pi]$. Here, φ_n and φ_m are statistically independent when $n \neq m$, so the condition in Eq. (13) is satisfied [45, 47]. By interpreting the modes in Eq. (17) as natural modes of oscillations of the source, our prescribed choice of a_n generates random sample pulses, which are linear combinations of fundamental fields with random phases. It is worth mentioning that the constructed field realizations have random fluctuations both in phase and amplitude, but that each random field realization contains the same amount of energy [23].

Propagation of GSM pulses in resonant nonlinear media can be simulated by applying the source pulse Eq. (13) into wave equations Eqs.(1)-(3) and Eqs.(6)-(7). As mentioned previously, each random realization will be propagated in the media individually. The process will be repeated many times for all different realizations of the field, and the resulting intensities will be averaged to produce a partially coherent pulse intensity according to Eq. (11).

4. Physical model of the source and host medium

We consider a GSM as a generic model of a random input pulse and proceed to generate an ensemble of source pulses according to the just outlined prescription. In Fig. 1, we exhibit

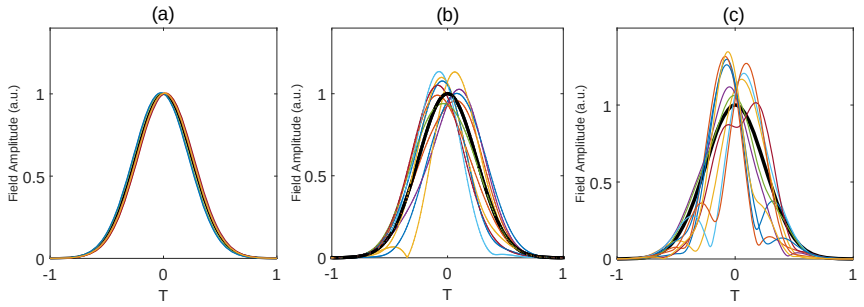

Fig. 1. Magnitude of 10 random field realizations of the GSM pulse at the source $Z = 0$ as a function of dimensionless time $T = t/t_p$ in three cases (a) $t_c = 10t_p$, (b) $t_c = 2t_p$ and (c) $t_c = t_p$. Black thick line: ensemble average amplitude.

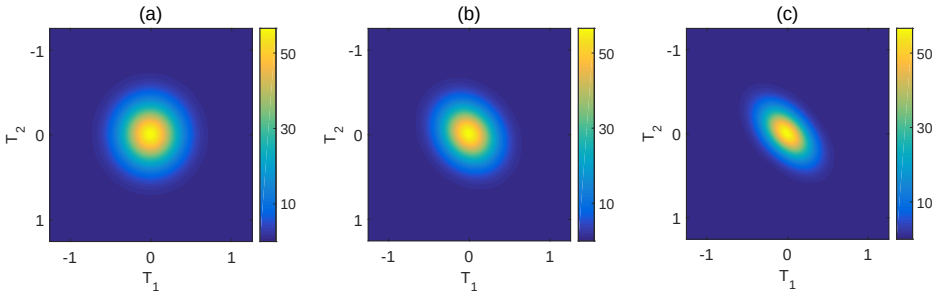

Fig. 2. Profile of the mutual coherence function at the source, $Z = 0$ as a function of dimensionless time T_1 and T_2 in three cases : (a) $t_c = 10t_p$, (b) $t_c = 2t_p$ and (c) $t_c = t_p$.

#249844 Received 9 Sep 2015; revised 4 Nov 2015; accepted 5 Nov 2015; published 11 Nov 2015

three short GSM pulses with different coherence level at the source: a relatively coherent input pulse with $t_c = 10t_p$, a moderately coherent pulse with $t_c = 2t_p$ and a relatively incoherent pulse with $t_c = t_p$. The magnitude of simulated sample pulses are presented in Fig. 1 for 10 random realizations. It can be seen in the figure that each field realization has random fluctuations which become progressively more pronounced as the pulse coherence level decreases. The averaged pulse amplitude for a large set of realizations is also displayed with thick black line. We also display the mutual coherence function profile at the source as a function of a pair of dimensionless time instances $T_1 = t_1/t_p$ and $T_2 = t_2/t_p$ in Fig. 2. It is seen in the figure that the relatively coherent pulse has a nearly isotropic mutual coherence function profile, while that of the relatively incoherent pulse is strongly anisotropic with a sharp peak along the diagonal $T_1 = T_2$. This behaviour naturally reflects δ-function like coherence properties of such pulses.

As mentioned in the previous section, the number of modes in the Karhunen-Loève decomposition of each ensemble member is relevant to the coherence level of the source pulse. Thus, we employ a large number of modes to faithfully represent relatively incoherent pulses through Eq. (13) [47]. At the same time, the Monte Carlo simulation accuracy crucially depends on the number of the sample field realizations, L. The ensemble average represented by Eq. (11), converges to the time average as the sample size L increases. Therefore, a high fluctuation level of relatively incoherent pulses–manifest in Fig. 1(c)–necessitates a high sample volume [23, 42].

The resonant host medium is modelled as a collection of two-level atoms. The two key relaxation rates–transverse and longitudinal–can be determined as follows. The total transverse relaxation rate is defined as [27]

$$\frac{1}{T_\perp} = \frac{1}{T_\perp^h} + \frac{1}{T_\perp^{in}}, \tag{24}$$

where $T_\perp^h$ and $T_\perp^{in}$ are homogenous and inhomogeneous broadening lifetimes, respectively. According to [48], the effective absorption line shape of the medium is affected by the ratio,

$$b = \sqrt{4\ ln2}\ \frac{\delta_h}{\delta_{in}}, \tag{25}$$

where $\delta_h = 1/T_\perp^h$ and $\delta_{in} = 1/T_\perp^{in}$ correspond to the homogenous and inhomogeneous linewidth, respectively. Eq.(25) distinguishes two limiting cases. In the first case, $\delta\nu_{in} >> \delta\nu_h$, the transverse decay rate is mainly due to inhomogeneous broadening. In contrast, if $\delta\nu_h >> \delta\nu_{in}$, the homogeneous broadening is dominant and the transverse decay rate is mostly influenced by collisions.

The energy relaxation time $T_{||}$, defining the time interval over which the atomic populations decay, is related to $T_\perp$ according to [1, 48];

$$\frac{1}{T_\perp} = \frac{1}{2T_{||}} + \frac{1}{T_\perp^h}. \tag{26}$$

In our simulations, we assume an inhomogeneously broadened medium such that $b \ll 1$. A dilute sodium vapour at $T = 300K$ with a density $N = 10^{11} cm^{-3}$ can serve as a physical realization of the medium. Setting $b = 0.05$, $T_{||} = 16$ ns, a typical value for the room temperature sodium [1], and $\delta_{in} = 1GHz$, and employing Eqs.(24) through (26), we obtain $T_\perp \simeq 32$ ns.

5. Numerical simulation results

We numerically study the evolution of random input pulse ensembles with the average pulse areas at the source $\mathscr{A}_0 = 0.8\pi$ and $\mathscr{A}_0 = 1.5\pi$ where the latter is defined, in dimensionless variables, as

$$\mathscr{A}(Z) \equiv \int_{-\infty}^{\infty} \sqrt{\langle I(T,Z)\rangle}\, dT; \tag{27}$$

#249844 Received 9 Sep 2015; revised 4 Nov 2015; accepted 5 Nov 2015; published 11 Nov 2015

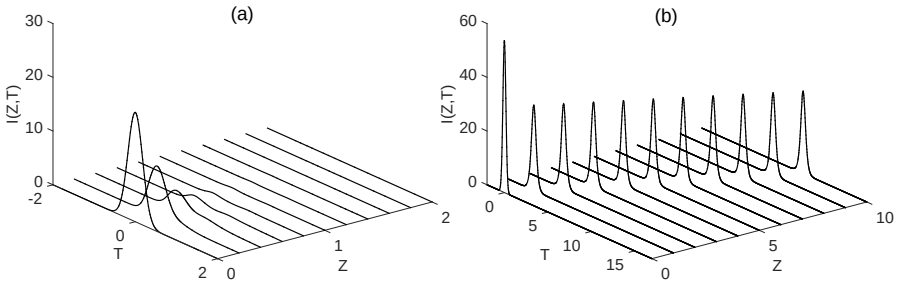

Fig. 3. Average intensity evolution of relatively coherent pulses as a function of the propagation distance Z. The cases (a) and (b) correspond to the average input pulse areas $\mathscr{A}_0 = 0.8\pi$ and $\mathscr{A}_0 = 1.5\pi$, respectively.

$\mathscr{A}_0 \equiv \mathscr{A}(0)$. It follows at once from Eq. (27) that the average area reduces to the standard pulse area [27] in the fully coherent limit.

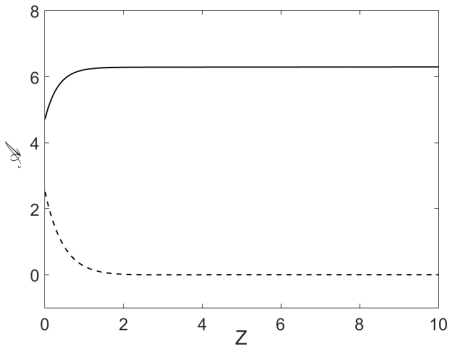

Fig. 4. Evolution of the average pulse area as a function of the propagation distance Z for relatively coherent pulses with $\mathscr{A}_0 = 0.8\pi$ (dashed) and, $\mathscr{A}_0 = 1.5\pi$ (solid), respectively.

We first examine the behaviour of relatively coherent input pulses with $t_c = 10t_p$. In Fig. 3, we illustrate the average intensity profile evolution of two such pulses with the areas $\mathscr{A}_0 = 0.8\pi$ and $\mathscr{A}_0 = 1.5\pi$ through the inhomogeneously broadened medium, corresponding to the cases Fig. 3(a) and 3(b) in the figure. We can see in Fig. 3(a) that a smaller area pulse suffers strong absorption on its propagation through the medium and no soliton formation is observed. Moreover, Fig. 4 represents the evolution of the average pulse area as a function of the propagation distance. It is evident from the figure that the corresponding pulse area, displayed with a dashed line, rapidly reaches zero upon pulse entrance into the medium. On the other hand, we can see in Fig. 3(b) that a larger area pulse initially broadens, while its peak intensity decreases. The pulse is, however, ultimately converted into a stable soliton which is evident in the figure: the pulse maintains its shape, suffering no visible attenuation over sufficiently large propagation distances. We notice also that all relatively coherent pulses experience a time delay on propagation which is manifested through the pulse intensity peak shift relative to its position at the source. As is seen in Fig. 4, the average pulse area, plotted with a solid line, attains the asymptotic value of 2π, reminiscent of the fully coherent self-induced transparency situation [27]. Thus, our results can be interpreted as the manifestation of self-induced transparency (SIT)

#249844 Received 9 Sep 2015; revised 4 Nov 2015; accepted 5 Nov 2015; published 11 Nov 2015

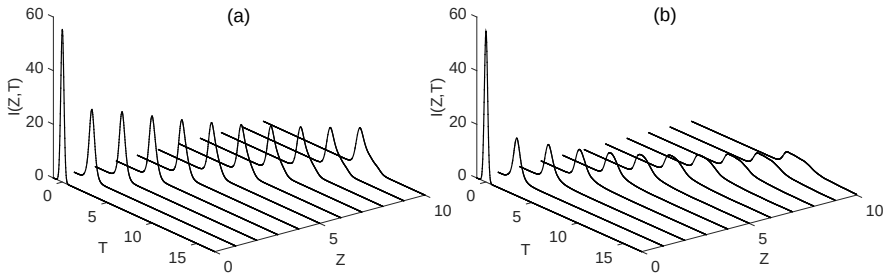

Fig. 5. Average intensity evolution as a function of propagation distance Z for input pulses with (a) $t_c = 2t_p$ and (b) $t_c = t_p$. The average pulse area at the source is $\mathscr{A}_0 = 1.5\pi$.

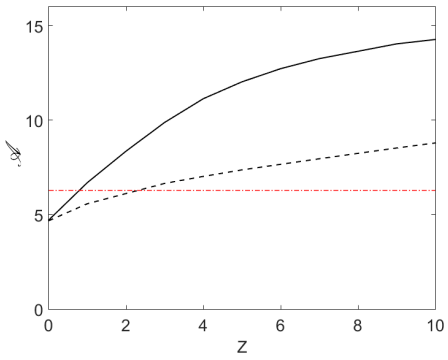

Fig. 6. Evolution of the averaged pulse area as a function of propagation distance Z, corresponding to $t_c = 2t_p$ (dashed line) and, $t_c = t_p$ (solid line) with the initial area $\mathscr{A}_0 = 1.5\pi$. The red dotted-dashed line represents the $\mathscr{A} = 2\pi$ limit.

phenomena and solitary-pulse formation in presence of small noise at the source.

To elucidate the influence of the input pulse coherence level on the SIT soliton formation, we also study the evolution of random pulses with lower levels of coherence. In Fig. 5, we illustrate the evolution of partially coherent ($t_c = 2t_p$) and rather incoherent ($t_c = t_p$) incident pulses with the initial area $\mathscr{A}_0 = 1.5\pi$. It can be seen in Fig. 5(a) that a partially coherent pulse intensity profile becomes wider and more shallow upon propagation. The pulse leading edge self-steepens, distorting its symmetry as well. The similar behaviour is exhibited by rather incoherent pulses, as is seen in Fig. 5(b). In this case, though, pulse broadening and peak intensity decrease are more pronounced. The average pulse area dynamics are shown in Fig. 6. It is seen in the figure that in both cases, the area appears to monotonously increase with the propagation distance, exceeding the value of 2π. We can infer that SIT soliton formation is precluded for the incident pulses with high enough fluctuation levels.

To explain the evolution scenario difference of more from less coherent input pulses, we recall that each statistical ensemble consists of a number of pulse realizations. As an example, in Fig. 7 we display the evolution of five relatively coherent random pulse realizations at three propagation distances: $Z = 0$, $Z = 5$ and $Z = 10$. As it is evident in the figure, the field realizations have almost the same initial area and, consequently nearly the same behaviour upon propagation. Thus upon averaging, such an ensemble yields a nearly coherent pulse transform-

#249844 Received 9 Sep 2015; revised 4 Nov 2015; accepted 5 Nov 2015; published 11 Nov 2015

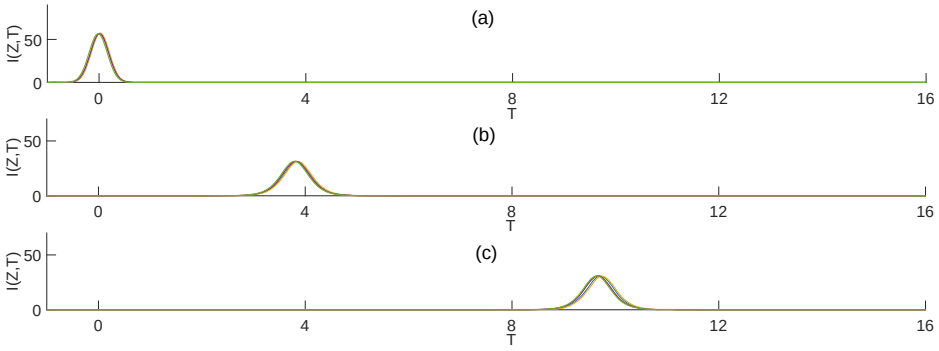

Fig. 7. Intensity of five relatively coherent, $t_c = 10t_p$, pulse realizations with $\mathscr{A}_0 = 1.5\pi$ at three sample points in Z: $Z = 0$ (a), $Z = 5$ (b), and $Z = 10$ (c), respectively.

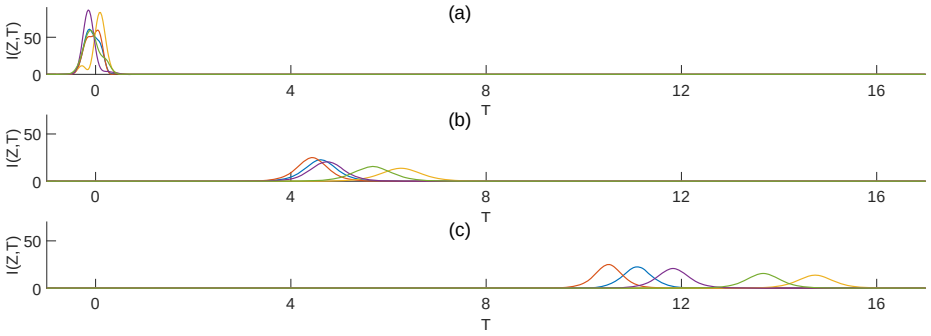

Fig. 8. Intensity of five rather incoherent, $t_c = t_p$ pulse realizations with $\mathscr{A}_0 = 1.5\pi$ at three sample points in Z: $Z = 0$ (a), $Z = 5$ (b), and $Z = 10$ (c), respectively.

ing to a SIT soliton. On the contrary, in a rather incoherent pulse case, ($t_c = t_p$), the ensemble realizations, shown in Fig. 8, vary greatly in their initial shape and area. As a result, different realizations suffer widely different time delays upon propagation as is seen in the figure. Notice also that the realization pulse distribution in Fig. 8 explains the output pulse asymmetry manifest in Fig. 5. The ensemble averaging then results in a long shallow pulse, more susceptible to incoherent relaxation processes that ultimately preclude the SIT soliton formation in this case.

Let us now focus on the mutual coherence function evolution in the system. In Fig. 9, we represent the mutual coherence function of the three pulses–a relatively coherent, partially coherent and nearly incoherent ones–at the source $Z = 0$ and at the distance $Z = 10$ away from the source. To obtain reliable results at the output, we used $L = 2000$ sample realizations for the nearly incoherent case and $L = 1000$ for the partially coherent case. We can infer from the figure that the mutual coherence function profiles in all cases become progressively more centred along the $T_1 = T_2$ diagonal, implying pulse coherence reduction upon their propagation in the medium. Moreover, the least coherent input pulses display the fastest coherence loss rate. Such a behaviour can be explained by recalling that relatively incoherent pulses broaden faster than do relatively coherent ones. Hence, the former become long enough to be affected by incoherent relaxation processes at shorter propagation distances than are the latter. Thus, less coherent pulses lose their coherence faster than do more coherent ones. However, regardless of the initial coherence level, all random pulses become progressively less coherent on propagation in

#249844 Received 9 Sep 2015; revised 4 Nov 2015; accepted 5 Nov 2015; published 11 Nov 2015

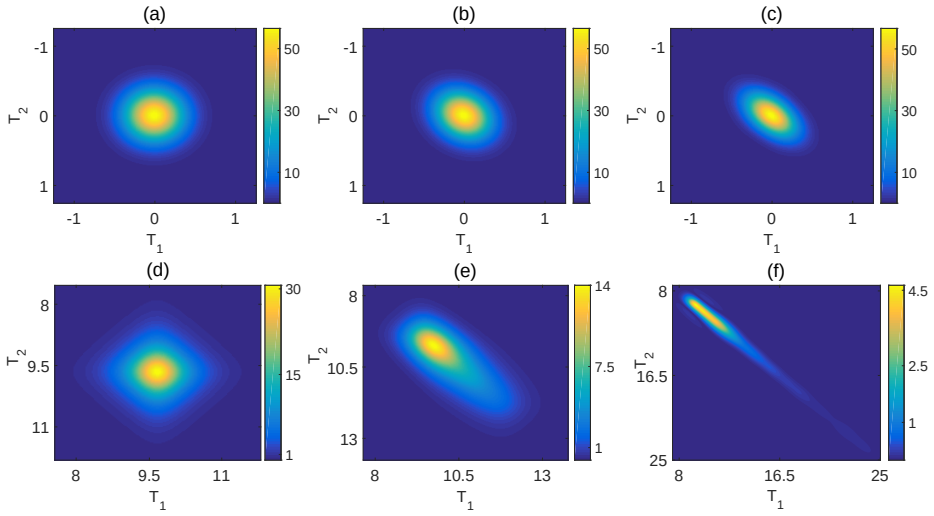

Fig. 9. Magnitude of the mutual coherence function at $Z = 0$, (top row) and $Z = 10$, (bottom row); $t_c = 10t_p$,(a,d); $t_c = 2t_p$, (b,e); $t_c = t_p$, (c,f).

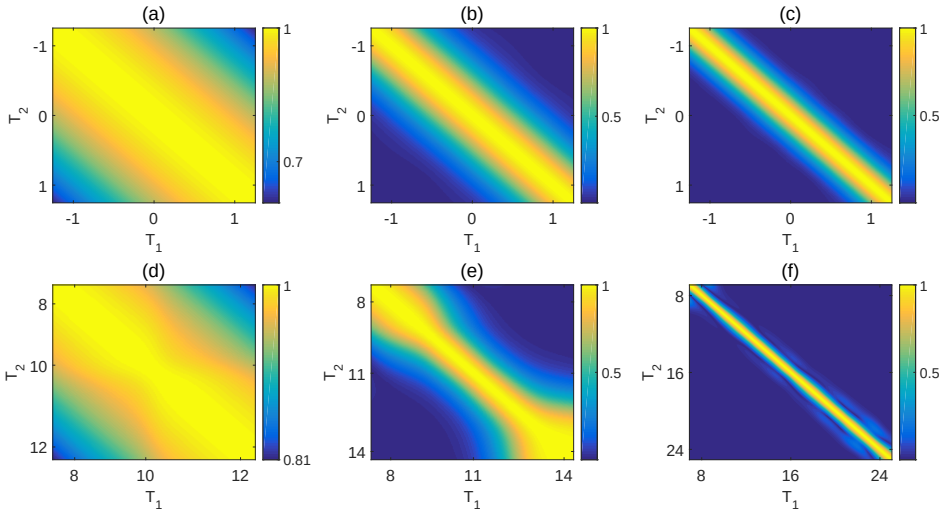

Fig. 10. Magnitude of the complex degree of coherence function at $Z = 0$, (top row) and $Z = 10$, (bottom row); $t_c = 10t_p$,(a,d); $t_c = 2t_p$, (b,e); $t_c = t_p$, (c,f).

resonant media due to the their temporal broadening which makes them subject to incoherent relaxation processes. The similar trend is reflected in the temporal degree of coherence evolution, exhibited in Fig. 10.

6. Conclusion

In summary, we applied numerical Monte Carlo techniques to simulate partially coherent GSM pulse propagation in a resonant, inhomogeneously broadened nonlinear medium. We modeled

#249844 Received 9 Sep 2015; revised 4 Nov 2015; accepted 5 Nov 2015; published 11 Nov 2015

the medium as a collection of two-level atoms. We numerically studied the dynamics of the ensemble averaged pulse intensity, the mutual coherence function, and the temporal degree of coherence as pulses of an arbitrary coherence state at the source propagate into the medium. We have elucidated conditions for self-induced transparency soliton formation in the system. Our simulation results reveal that self-induced transparency is possible provided the input pulses are sufficiently coherent and possess large enough average areas. We have also demonstrated that regardless of their initial state of coherence, random pulses lose their coherence on propagation. However, low-coherence input pulses lose their coherence at a faster rate than do their more coherent counterparts because the former broaden faster than the latter, and hence become susceptible to incoherent relaxation processes at shorter propagation distances than are the latter.

#249844 Received 9 Sep 2015; revised 4 Nov 2015; accepted 5 Nov 2015; published 11 Nov 2015